

BabyMamba-HAR: Lightweight Selective State Space Models for Efficient Human Activity Recognition on Resource Constrained Devices

Mridankan Mandal

Department of Information Technology
 Indian Institute of Information Technology, Allahabad
 Prayagraj, India
 mridankanmandal2006@gmail.com

Abstract—Human activity recognition (HAR) on wearable and mobile devices is constrained by memory footprint and computational budget, yet competitive accuracy must be maintained across heterogeneous sensor configurations. Selective state space models (SSMs) offer linear time sequence processing with input dependent gating, presenting a compelling alternative to quadratic complexity attention mechanisms. However, the design space for deploying SSMs in the TinyML regime remains largely unexplored. In this paper, BabyMamba-HAR is introduced, a framework comprising two novel lightweight Mamba inspired architectures optimized for resource constrained HAR: (1) CI-BabyMamba-HAR, using a channel independent stem that processes each sensor channel through shared weight, but instance independent transformations to prevent cross channel noise propagation, and (2) Crossover-BiDir-BabyMamba-HAR, using an early fusion stem that achieves channel count independent computational complexity. Both variants incorporate weight tied bidirectional scanning and lightweight temporal attention pooling. Through evaluation across eight diverse benchmarks, it is demonstrated that Crossover-BiDir-BabyMamba-HAR achieves 86.52% average macro F1-score with approximately 27K parameters and 2.21M MACs, matching TinyHAR (86.16%) while requiring 11 \times fewer MACs on high channel datasets. Systematic ablation studies reveal that bidirectional scanning contributes up to 8.42% F1-score improvement, and gated temporal attention provides up to 8.94% F1-score gain over mean pooling. These findings establish practical design principles for deploying selective state space models as efficient TinyML backbones for HAR.

Index Terms—Human Activity Recognition, TinyML, State Space Models, Mamba, Efficient sequence modeling, Wearable computing

I. INTRODUCTION

Human activity recognition (HAR) constitutes a foundational capability for mobile health monitoring, assistive technologies, and industrial safety systems, where motion patterns must be classified from multi-channel inertial sensor streams in real time. The deployment of HAR models on resource constrained wearable devices is strongly motivated by privacy considerations, raw sensor data can reveal sensitive behavioral patterns, and by latency requirements in safety critical applications. However, battery powered embedded systems impose severe constraints on model size (typically <100KB Flash) and computational cost (typically <10M MACs per inference),

which has catalyzed the development of TinyML oriented HAR architectures [5], [6], [8].

A persistent challenge in this domain is maintaining both efficiency and accuracy across heterogeneous benchmarks, where channel counts range from 3 (smartphone accelerometer) to 79 (full body sensor network), sampling rates vary from 20 Hz to 100 Hz, and sensor placement introduces varying correlation and noise structures. Furthermore, inconsistent evaluation protocols across prior work have obscured true model trade-offs [9], necessitating unified comparative studies.

Selective state space models (SSMs) have emerged as a promising paradigm for efficient sequence modeling. The Mamba architecture [1] introduces input dependent discretization that enables selective state updates with linear time complexity $O(N)$, contrasted with the $O(N^2)$ complexity of self attention mechanisms [3]. This property aligns naturally with HAR, where discriminative information is often localized in brief motion transitions while extended stationary periods contribute primarily noise.

Despite this alignment, the design space for lightweight SSMs in HAR remains insufficiently characterized. Critical questions include: (1) How should multi-channel sensor streams be projected into the state space backbone? (2) How should bidirectionality be implemented for windowed classification without doubling parameters? (3) Which temporal aggregation strategies remain robust under extreme parameter constraints?

These questions are addressed through a systematic study of two novel BabyMamba-HAR architectures evaluated under a unified protocol across eight public datasets. The contributions of this work are:

- Two complementary lightweight SSM architectures: CI-BabyMamba-HAR with channel independent processing for noise robustness, and Crossover-BiDir-BabyMamba-HAR with early fusion for computational efficiency on high channel datasets.
- A weight tied bidirectional scanning mechanism that doubles the effective receptive field without additional parameters.

- A lightweight context gated temporal attention pooling head that focuses on discriminative timesteps.
- Evaluation across eight benchmarks with unified preprocessing, subject independent splits, and five random seed statistical reporting.
- Systematic ablation studies isolating the contribution of bidirectionality, pooling strategy, stem architecture, and model hyperparameters.

II. RELATED WORK

A. Efficient HAR Architectures

Lightweight HAR has been extensively studied through CNN and RNN compression techniques. DeepConvLSTM [4] established the CNN-LSTM paradigm, achieving strong accuracy, but requiring $>130K$ parameters. TinyHAR [5] introduced compact 2D convolutions with temporal attention pooling, reducing parameters to $\sim 55K$ while maintaining competitive accuracy. TinierHAR [6] further compressed models to $\sim 33K$ parameters using depthwise separable convolutions and bidirectional GRU. Additional efficiency oriented designs include knowledge distillation approaches [10], neural architecture search for mobile deployment [11], and MLP only backbones [12].

Transformer based HAR models have also been investigated, but their quadratic complexity with sequence length raises concerns for resource constrained deployment [13]. Recent work on cross dataset generalization [14] and evaluation protocol standardization [9] has highlighted the importance of unified benchmarking.

B. State Space Models and Mamba

State space models provide a principled framework for sequence modeling through structured linear recurrences. The S4 architecture [2] demonstrated efficient long range dependency modeling through HiPPO initialized state matrices. Mamba [1] introduced selective state spaces where discretization parameters become input dependent, enabling content-aware gating with hardware efficient parallel scans.

Recent work has begun adapting Mamba to sensor based HAR. In HARMamba [15], a bidirectional Mamba architecture for wearable sensors was proposed. However, existing SSM based HAR designs have not systematically characterized the lightweight regime ($<30K$ parameters) nor provided controlled ablations isolating architectural contributions.

III. METHODOLOGY

A. Problem Formulation

Consider a multi-channel inertial sensor window $\mathbf{X} \in \mathbb{R}^{C \times L}$, where C denotes the number of sensor channels and L the sequence length in timesteps. The objective is to predict an activity label $y \in \{1, \dots, K\}$ for K classes. A feature backbone maps the input to a latent sequence $\mathbf{Z} \in \mathbb{R}^{L \times d_{\text{model}}}$, followed by temporal aggregation to produce a fixed dimensional representation for classification.

B. Selective State Space Formulation

The continuous time linear state space model is defined as:

$$\frac{dh(t)}{dt} = \mathbf{A}h(t) + \mathbf{B}x(t) \quad (1)$$

$$y(t) = \mathbf{C}h(t) + \mathbf{D}x(t) \quad (2)$$

where $h(t) \in \mathbb{R}^N$ is the latent state, and $\mathbf{A} \in \mathbb{R}^{N \times N}$, $\mathbf{B} \in \mathbb{R}^{N \times d}$, $\mathbf{C} \in \mathbb{R}^{d \times N}$, $\mathbf{D} \in \mathbb{R}^{d \times d}$ are learnable parameters. Discretization through zero order hold with step size Δ yields:

$$h_t = \bar{\mathbf{A}}h_{t-1} + \bar{\mathbf{B}}x_t \quad (3)$$

$$y_t = \mathbf{C}h_t + \mathbf{D}x_t \quad (4)$$

where $\bar{\mathbf{A}} = \exp(\Delta \mathbf{A})$ and $\bar{\mathbf{B}} = (\Delta \mathbf{A})^{-1}(\exp(\Delta \mathbf{A}) - \mathbf{I})\Delta \mathbf{B}$.

The Mamba selective mechanism [1] makes Δ_t , \mathbf{B}_t , and \mathbf{C}_t input dependent:

$$\Delta_t = \text{softplus}(\mathbf{W}_{\Delta}x_t) \quad (5)$$

$$\mathbf{B}_t = \mathbf{W}_Bx_t, \quad \mathbf{C}_t = \mathbf{W}_Cx_t \quad (6)$$

This selectivity enables the model to dynamically gate state updates: small Δ_t preserves history, while large Δ_t encourages forgetting. For HAR, this allows selective attention to motion transitions while suppressing stationary noise.

C. BabyMamba-HAR Architecture Family

Two complementary architectures are proposed, addressing distinct sensor configuration scenarios through different stem designs.

1) *CI-BabyMamba-HAR (Channel Independent)*: The channel independent architecture (Fig. 1) addresses noise isolation in heterogeneous sensor arrays. Each sensor channel is processed independently through a shared convolutional stem, enabling noise isolation between heterogeneous sensors while maintaining parameter efficiency through weight sharing. The processed channels flow through stacked weight tied bidirectional SSM blocks, where forward and backward scans share parameters to double the receptive field without increasing model size. This architecture is particularly suited for datasets with heterogeneous or noisy sensor configurations where cross channel interference must be minimized. Each channel $\mathbf{X}^{(c)} \in \mathbb{R}^{1 \times L}$ is processed through a shared convolutional stem:

$$\mathbf{Z}^{(c)} = \sigma(\text{BN}(\text{Conv1d}(\mathbf{X}^{(c)}; \mathbf{W}_{\text{stem}}))) \quad (7)$$

where $\mathbf{W}_{\text{stem}} \in \mathbb{R}^{d_{\text{model}} \times 1 \times k}$ are shared weights and $\sigma(\cdot)$ is SiLU activation. The backbone processes $B \cdot C$ independent sequences, and late fusion averages channel representations:

$$\mathbf{h} = \frac{1}{C} \sum_{c=1}^C \text{pool}(\phi_{\text{ssm}}(\mathbf{Z}^{(c)})) \quad (8)$$

Configuration: $d_{\text{model}} = 24$, $d_{\text{state}} = 16$, $n_{\text{layers}} = 4$, $\text{expand} = 2$, yielding $\sim 28K$ parameters.

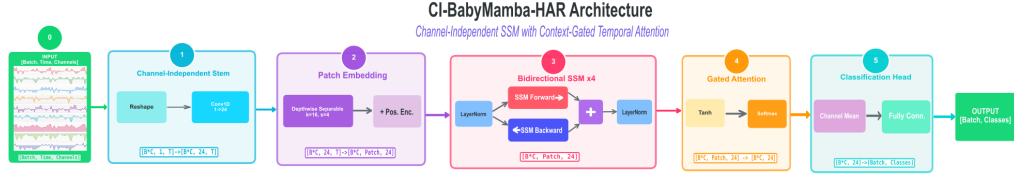


Fig. 1. CI-BabyMamba-HAR architecture. The channel independent stem processes each sensor channel through shared weight Conv1D, BatchNorm, and SiLU layers. Weight tied bidirectional SSM blocks enable forward and backward temporal processing. A context gated temporal attention head aggregates features before classification.

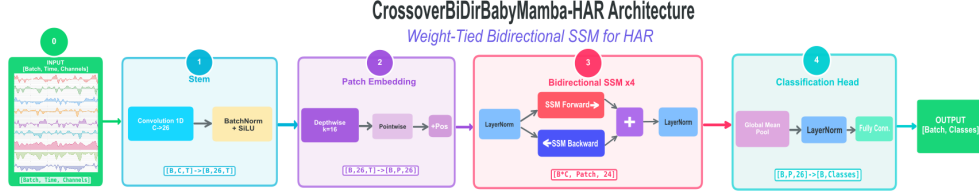


Fig. 2. Crossover-BiDir-BabyMamba-HAR architecture. The early fusion stem projects all input channels to d_{model} features through a single Conv1D operation. Bidirectional SSM blocks with crossover connections process the fused representation. Backbone computational complexity is independent of input channel count.

2) *Crossover-BiDir-BabyMamba-HAR (Early Fusion)*: The early fusion architecture (Fig. 2) achieves channel count independent complexity through immediate projection. All C input channels are fused into d_{model} features through a single convolution operation, and the crossover mechanism facilitates information exchange between forward and backward processing paths in the bidirectional SSM blocks. This design is particularly efficient on high channel datasets such as Opportunity (79 channels), where $11 \times$ fewer MACs are achieved compared to conventional architectures while maintaining competitive accuracy.

$$\mathbf{Z} = \sigma(\text{BN}(\text{Conv1d}(\mathbf{X}; \mathbf{W}_{\text{fused}}))) \quad (9)$$

where $\mathbf{W}_{\text{fused}} \in \mathbb{R}^{d_{\text{model}} \times C \times k}$ maps C channels to d_{model} dimensions. The backbone processes only B sequences regardless of C , yielding:

$$\text{MACs}_{\text{Crossover}} = \frac{\text{MACs}_{\text{SCI}}}{C} \quad (10)$$

Configuration: $d_{\text{model}} = 26$, $d_{\text{state}} = 8$, $n_{\text{layers}} = 4$, $\text{expand} = 2$, yielding $\sim 27\text{K}$ parameters.

3) *Weight Tied Bidirectional Scanning*: Windowed HAR classification has access to the complete input sequence, eliminating causality constraints. Bidirectional context is introduced through weight tied forward and backward scans (Fig. 3). The Mamba inspired selective mechanism makes the discretization step Δ_t and state matrices \mathbf{B}_t , \mathbf{C}_t input dependent through learned linear projections, enabling dynamic control of information flow: small Δ_t values preserve historical context while large values encourage selective forgetting. This content aware gating is particularly beneficial for HAR, where discriminative

motion transitions are brief while stationary periods contribute primarily noise. The formulation is as follows:

$$\mathbf{H}_{\text{fwd}} = \text{SSM}_{\theta}(\mathbf{Z}) \quad (11)$$

$$\mathbf{H}_{\text{bwd}} = \mathcal{T}(\text{SSM}_{\theta}(\mathcal{T}(\mathbf{Z}))) \quad (12)$$

$$\mathbf{Z}_{\text{out}} = \text{LN}(\mathbf{Z} + \mathbf{H}_{\text{fwd}} + \mathbf{H}_{\text{bwd}}) \quad (13)$$

where \mathcal{T} denotes temporal reversal and θ are shared parameters. This doubles the effective receptive field without parameter increase.

4) *Context Gated Temporal Attention Pooling*: Global average pooling treats all timesteps equally, diluting brief discriminative segments. Learnable attention is employed:

$$\mathbf{e}_t = \tanh(\mathbf{W}_g \mathbf{z}_t + \mathbf{b}_g) \quad (14)$$

$$\alpha_t = \frac{\exp(\mathbf{v}^{\top} \mathbf{e}_t)}{\sum_{j=1}^L \exp(\mathbf{v}^{\top} \mathbf{e}_j)} \quad (15)$$

$$\mathbf{c} = \sum_{t=1}^L \alpha_t \mathbf{z}_t \quad (16)$$

This adds only $d_{\text{model}} \times d_{\text{attn}} + 2d_{\text{attn}} \approx 624$ parameters.

D. Computational Complexity

The SSM backbone has complexity $O(L \cdot d_{\text{model}} \cdot d_{\text{state}})$, linear in sequence length. For Crossover-BiDir-BabyMamba-HAR, backbone compute is independent of C . For CI-BabyMamba-HAR, complexity scales as $O(L \cdot C \cdot d_{\text{model}} \cdot d_{\text{state}})$. This distinction is critical for high channel datasets.

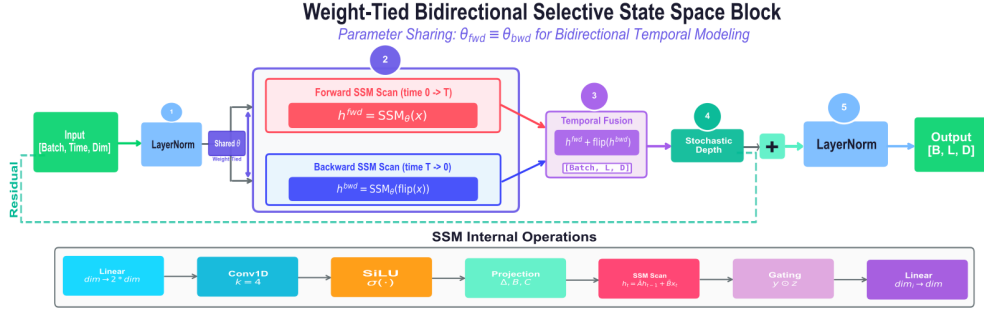


Fig. 3. Weight tied Bidirectional Selective state space (SSM) block architecture. Input dependent projections control discretization step Δ_t and state matrices \mathbf{B}_t , \mathbf{C}_t . The parallel scan implementation maintains linear time complexity $O(N)$.

IV. EXPERIMENTAL SETUP

A. Evaluation Protocol

To ensure fair comparison, all models share identical data loading pipelines, metric computation (macro F1-score), and random seed control. Subject independent splits followed dataset author specifications where available, otherwise, leave one subject out cross-validation (LOSO CV) was applied. Results are reported as mean \pm standard deviation over five seeds generated from a master seed.

A critical methodological consideration arises for single subject datasets where standard subject-wise splitting is inapplicable. The Skoda dataset [24] presents a particularly instructive case: with only one participant performing industrial assembly activities in a manufacturing environment, naive random splitting of overlapping windows induces severe data leakage, as adjacent windows share 75% of their samples. To address this, a *temporal split* is used strategy within each activity class, the first 80% of chronologically ordered windows are assigned to training and the remaining 20% to testing. This protocol ensures that test samples are temporally disjoint from training data, preventing artificially inflated performance metrics that would otherwise arise from near duplicate samples spanning the train-test boundary.

B. Dataset Specific Preprocessing

Dataset preprocessing was tailored to sensor characteristics:

- **Standard preprocessing** (UCI-HAR, MotionSense, WISDM, Opportunity, UniMiB, Daphnet): Per-channel z-score normalization ($x' = (x - \mu_c)/\sigma_c$) computed on training data.
- **Signal rescue** (PAMAP2): Robust scaling (median/IQR) to handle hardware artifacts from intentionally loose sensors, combined with 5 Hz Butterworth low-pass filtering to remove high frequency noise while preserving activity signatures.
- **Signal rescue** (Skoda): 5 Hz low-pass Butterworth filter to suppress industrial vibration artifacts from the assembly line environment, followed by z-score normalization. Overlapping windows (75% overlap, stride=24 for 98-

TABLE I
DATASET CHARACTERISTICS AND WINDOWING CONFIGURATION.

Dataset	Subj.	Classes	Ch.	Hz	L	Sec.
UCI-HAR [18]	30	6	9	50	128	2.56
MotionSense [19]	24	6	6	50	128	2.56
WISDM [20]	36	6	3	20	128	6.40
PAMAP2 [21]	9	12	19	100	128	1.28
Opportunity [22]	4	5	79	30	128	4.27
UniMiB-SHAR [23]	30	9	3	50	128	2.56
Skoda [24]	1	11	30	98	98	1.00
Daphnet [25]	10	2	9	64	64	1.00

sample windows) are employed to augment the limited single-subject data.

All filtering used 4th order Butterworth design with zero phase forward-backward application to prevent temporal distortion.

C. Datasets

Eight public benchmarks spanning diverse sensor modalities were evaluated (Table I).

D. Training Configuration

Models were trained with AdamW optimizer [7] ($\beta_1 = 0.9$, $\beta_2 = 0.999$), learning rate scheduler (ReduceLROnPlateau, factor=0.5, patience=5), and early stopping (patience=10 on validation F1-score). Maximum epochs: 200. Gradient clipping: max_norm=1.0. Loss: CrossEntropy with label smoothing $\epsilon = 0.1$.

Online data augmentation included time warping ($p = 0.5$), magnitude scaling ($p = 0.5$, $\alpha \sim \mathcal{U}(0.8, 1.2)$), Gaussian jitter ($p = 0.3$, $\sigma = 0.05$), and channel dropout ($p = 0.2$).

E. Baselines

All baselines were re-implemented in the unified codebase: TinyHAR [5] ($\sim 55K$ params), TinierHAR [6] ($\sim 33K$ params), and DeepConvLSTM [4] ($\sim 136K$ params).

V. RESULTS

A. Overall Performance Comparison

Table II presents macro F1-scores across all datasets. Crossover-BiDir-BabyMamba-HAR achieves 86.52% average

BabyMamba-HAR Models and Baselines Comparison

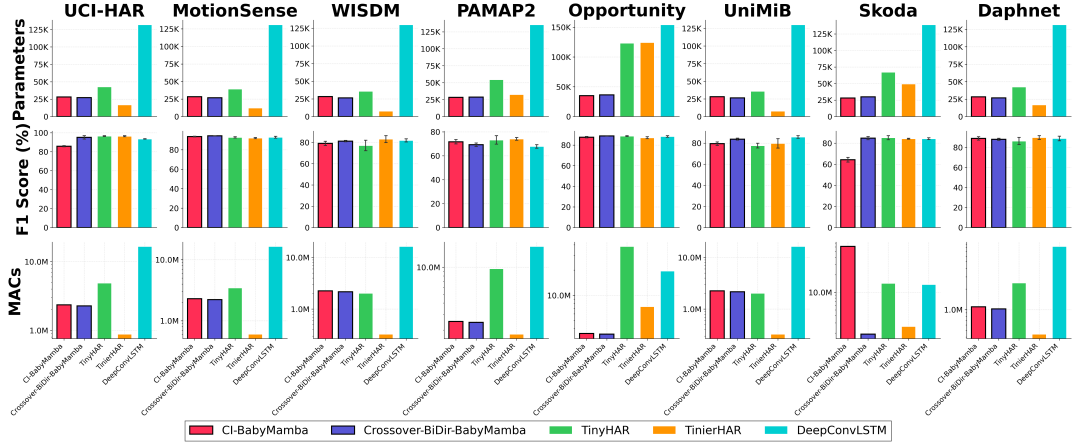


Fig. 4. Performance comparison grid across all eight HAR benchmark datasets showing macro F1-scores for each model-dataset combination.

F1-score, comparable to TinyHAR (86.16%), and within 0.87 points of TinierHAR (87.39%), while maintaining $\sim 27K$ parameters.

B. Computational Efficiency

Table III summarizes computational costs. Crossover-BiDir-BabyMamba-HAR achieves $11\times$ fewer MACs than TinyHAR on Opportunity (3.44M vs. 38.30M MACs) while matching F1-score (88.81% vs. 88.69%). CI-BabyMamba-HAR's MACs scale with channel count, reaching 222M MACs on Opportunity (79 channels), making it impractical for high dimensional datasets.

C. High Channel Dataset Analysis

On Opportunity (79 channels) and Skoda (30 channels), the Crossover-BiDir architecture's channel independent compute is decisive:

A visualization of performance across all eight datasets is presented in Fig. 4. As shown, Crossover-BiDir-BabyMamba-HAR demonstrates consistent strong performance across diverse sensor configurations, achieving the highest F1-scores on MotionSense (93.03%) and Opportunity (88.81%). Notably, on Skoda, where the temporal splitting protocol eliminates data leakage from overlapping windows, TinyHAR achieves 85.22% F1-score compared to Crossover-BiDir-BabyMamba's 84.74%. This modest gap contrasts sharply with pre-correction results where both models exceeded 97%, underscoring the importance of rigorous evaluation protocols for single-subject datasets. The contrasting performance profiles between CI-BabyMamba-HAR and Crossover-BiDir-BabyMamba-HAR show the importance of stem architecture selection based on dataset characteristics: early fusion excels when channels exhibit high correlation, while channel independent processing provides robustness for heterogeneous sensor arrays.

VI. ABLATION STUDIES

Systematic ablations isolate architectural contributions using controlled single variable experiments. All ablations report mean \pm std over 5 seeds.

A. Bidirectionality Impact

Table V demonstrates that bidirectional scanning is critical for complex temporal patterns (MotionSense: -8.42% F1-score, PAMAP2: -6.32% F1-score), while simpler datasets (UCI-HAR) show minimal impact. The Crossover architecture is more robust to unidirectional ablation, likely due to the crossover mechanism providing implicit redundancy.

B. Temporal Pooling Strategy

Gated temporal attention provides considerable improvements for CI-BabyMamba-HAR (Table VI), with up to 8.94% F1-score gain on MotionSense. This confirms that learnable attention is essential for focusing on discriminative temporal segments.

C. Channel Processing Strategy

The C2 ablation evaluating explicit channel independent processing was completed across all eight datasets for both architectures (80 total runs: 8 datasets \times 2 models \times 5 seeds). Table VII summarizes key findings.

Crossover's early fusion dominates on 7 out of 8 datasets, with gains of +19% on Skoda and +10% on Opportunity. The sole exception is PAMAP2, where intentional sensor artifacts favor channel isolation. This evaluation confirms that stem architecture should prioritize fusion for correlated sensors and isolation only when independent noise profiles exist.

D. Hyperparameter Sensitivity

Table VIII indicates remarkable robustness to hyperparameter variation. Reducing d_{state} from 16 to 8 saves 16% parameters with $<0.5\%$ F1-score impact, enabling sub-25K parameter deployments. Increasing expansion factor to 3 adds

TABLE II

MACRO F1-SCORE (%) COMPARISON ACROSS ALL DATASETS. BEST RESULT PER DATASET IN **BOLD**. PARAMETER COUNTS AND MACs VARY BY DATASET DUE TO INPUT CHANNEL DIFFERENCES.

Model	UCI-HAR	Motion.	WISDM	PAMAP2	Opport.	UniMiB	Skoda	Daphnet	Avg
Crossover-BiDir-BabyMamba	95.13 \pm 1.79	93.03 \pm 0.49	80.69 \pm 1.44	65.67 \pm 2.71	88.81 \pm 0.28	83.74 \pm 0.93	84.74 \pm 1.50	88.08 \pm 1.07	85.02
CI-BabyMamba-HAR	84.79 \pm 0.39	86.21 \pm 1.50	77.76 \pm 2.40	65.46 \pm 2.52	76.73 \pm 1.76	80.83 \pm 2.97	64.34 \pm 2.23	84.59 \pm 0.79	77.59
TinyHAR [5]	96.53 \pm 0.41	92.67 \pm 0.67	77.09 \pm 4.95	73.22 \pm 3.58	88.69 \pm 0.38	77.61 \pm 2.23	85.22 \pm 1.91	86.42 \pm 3.64	86.01
TimierHAR [6]	96.37 \pm 0.57	91.99 \pm 0.60	83.06 \pm 3.24	74.07 \pm 1.16	87.09 \pm 0.90	79.67 \pm 4.45	84.21 \pm 0.47	89.84 \pm 1.90	85.85
DeepConvLSTM [4]	93.53 \pm 0.26	92.90 \pm 0.96	81.84 \pm 1.46	67.79 \pm 1.50	88.30 \pm 0.72	85.83 \pm 1.22	84.27 \pm 0.88	88.95 \pm 2.26	85.42

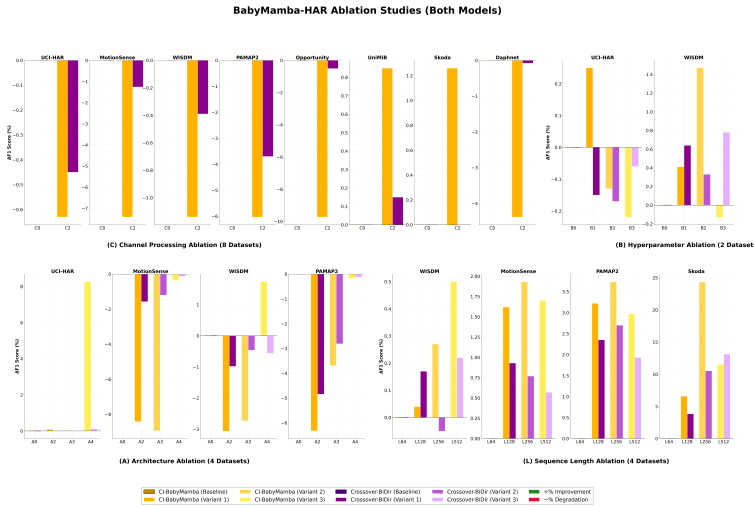


Fig. 5. Combined ablation study results showing $\Delta F1$ relative to baseline configurations. (C) Channel processing ablation across all 8 datasets comparing CI-BabyMamba vs. Crossover architectures with channel independent stem variants. (B) Hyperparameter sensitivity (d_{state} , d_{model} , expand factor) on 2 representative datasets. (A) Architecture ablation (bidirectionality A2, pooling A3, stem A4) on 4 datasets. (L) Sequence length scaling (64–512 timesteps) on 4 datasets. Yellow/gold bars: CI-BabyMamba-HAR, and purple bars: Crossover-BabyMamba-HAR. Baseline variants (A0, B0, C0, L64) shown with bold outlines.

TABLE III
COMPUTATIONAL EFFICIENCY COMPARISON (AVERAGED ACROSS DATASETS).

Model	Params	Avg MACs	F1/M-MACs
Crossover-BiDir-BabyMamba	27K	2.21M	39.1
CI-BabyMamba-HAR	28K	50.92M	1.6
TinyHAR	55K	9.29M	9.3
TimierHAR	33K	1.73M	50.5
DeepConvLSTM	136K	15.51M	5.5

TABLE IV
PERFORMANCE ON HIGH CHANNEL DATASETS.

Dataset	Model	F1 (%)	MACs	Speedup
Opportunity	Crossover-BabyMamba	88.81	3.44M	11.1 \times
	TinyHAR	88.69	38.30M	1.0 \times
	CI-BabyMamba	76.73	222.31M	0.17 \times
Skoda	Crossover-BabyMamba	84.74	1.92M	6.0 \times
	TinyHAR	85.22	11.48M	1.0 \times
	DeepConvLSTM	84.27	13.39M	0.86 \times

44% parameters without benefit, confirming that lightweight models are not capacity limited.

E. Key Ablation Findings

The ablation results are visualized in Fig. 5. Key findings:

TABLE V
ABLATION: BIDIRECTIONAL VS. UNIDIRECTIONAL SCANNING.

Dataset	Model	BiDir F1 (%)	UniDir F1 (%)
MotionSense	CI-BabyMamba-HAR	93.47	85.05 (-8.42)
	Crossover-BabyMamba	94.31	92.74 (-1.57)
PAMAP2	CI-BabyMamba-HAR	71.67	65.35 (-6.32)
	Crossover-BabyMamba	69.20	64.36 (-4.84)
UCI-HAR	CI-BabyMamba-HAR	85.80	85.88 (+0.08)
	Crossover-BabyMamba	95.11	95.10 (-0.01)

TABLE VI
ABLATION: GATED ATTENTION VS. MEAN POOLING.

Dataset	Model	Gated Attn F1 (%)	Mean Pool F1 (%)
MotionSense	CI-BabyMamba	93.47	84.53 (-8.94)
	Crossover-BabyMamba	94.31	93.11 (-1.20)
PAMAP2	CI-BabyMamba	71.67	67.98 (-3.69)
	Crossover-BabyMamba	69.20	66.39 (-2.81)

- Bidirectionality is essential:** Up to 8.42% F1-score gain on MotionSense. Activities with asymmetric temporal signatures (sit to stand versus stand to sit) benefit from both forward and backward context.
- Gated attention is critical for CI-BabyMamba-HAR:**

TABLE VII
ABLATION: CHANNEL PROCESSING ACROSS ALL DATASETS (C2 VARIANT).

Dataset	CI-BabyMamba	Crossover-BiDir	Winner
UCI-HAR	85.17%	94.66%	Crossover-BiDir (+9.49)
MotionSense	86.06%	93.05%	Crossover-BiDir (+6.99)
WISDM	77.85%	80.78%	Crossover-BiDir (+2.93)
PAMAP2	65.64%	65.50%	CI-BabyMamba (+0.14)
Opportunity	77.86%	88.30%	Crossover-BiDir (+10.44)
UniMiB	80.28%	83.89%	Crossover-BiDir (+3.61)
Skoda	65.60%	84.74%	Crossover-BiDir (+19.14)
Daphnet	84.60%	88.00%	Crossover-BiDir (+3.40)

TABLE VIII
ABLATION: HYPERPARAMETER SENSITIVITY SUMMARY.

Parameter	Avg $\Delta F1$	Δ Params
d_{state} : 16 \rightarrow 8	<0.5%	-16%
d_{model} : 26 \rightarrow 24	<0.5%	-12%
expand: 2 \rightarrow 3	<1%	+44%
seq_len: 128 \rightarrow 64	-2%	0%

Up to 8.94% F1-score improvement. Channel independent processing requires learnable aggregation to focus on discriminative timesteps.

- 3) **Early fusion is generally superior:** C2 ablation across all 8 datasets shows Crossover-BiDir-BabyMamba-HAR outperforming CI-BabyMamba-HAR on 7/8 benchmarks (Table VII), often by large margins (+19% Skoda, +10% Opportunity). Only PAMAP2 shows marginal CI advantage (+0.14%), suggesting channel isolation benefits only datasets with explicit sensor artifacts.
- 4) **Hyperparameters are robust:** d_{state} reduction (16 \rightarrow 8) saves 16% parameters at <0.5% F1-score cost. Expand factor increase provides no benefit despite +44% parameters.

VII. DISCUSSION

A. Architecture Selection Guidelines

The evaluation yields actionable deployment guidelines: (1) **High channel count** ($C > 30$): Crossover-BiDir-BabyMamba-HAR achieves 11 \times fewer MACs than TinyHAR on Opportunity while matching F1-score, as backbone complexity is channel independent. (2) **Heterogeneous sensors**: CI-BabyMamba-HAR isolates per-channel noise, preferred when sensors have independent noise profiles (PAMAP2). (3) **Extreme constraints**: Crossover-BiDir-BabyMamba-HAR with $d_{state} = 8$ achieves sub-25K parameters and <3M MACs. (4) **Correlated features**: Early fusion strongly favored for pre-computed features (UCI-HAR: +9.49% F1-score with Crossover-BiDir-BabyMamba-HAR).

B. Efficiency and Scalability

The channel independent complexity of Crossover-BiDir-BabyMamba-HAR is decisive for emerging high density sensor networks. Full body motion capture (50–100 channels) renders CI architectures impractical (222M MACs on Opportunity), while Crossover-BiDir variant maintains constant

backbone cost regardless of C . The $O(N)$ sequence complexity of SSMs versus $O(N^2)$ attention further advantages BabyMamba-HAR for longer windows.

C. Key Design Insights

The ablations reveal that bidirectional scanning contributes up to 8.42% F1-score for complex temporal patterns, validating non-causal processing for windowed classification. The weight tied mechanism doubles receptive field without parameter overhead. Stem architecture choice is data dependent: C2 ablation across all 8 datasets confirms fusion superiority on 7 out of 8 benchmarks, with channel isolation beneficial only for explicitly noisy sensor configurations.

D. Limitations

Key limitations include: (1) bidirectional design precludes true streaming inference, (2) extreme class imbalance (Daphnet: >90% negative) may benefit from focal loss, (3) evaluation limited to inertial modalities, and (4) quantization effects on microcontrollers remain uncharacterized. Future work includes streaming compatible variants, mixed stem routing, and INT8 quantization studies.

VIII. CONCLUSION

In this work, BabyMamba-HAR is presented, as a framework of two novel lightweight selective state space architectures for efficient human activity recognition. CI-BabyMamba-HAR provides noise robustness through channel independent processing, while Crossover-BiDir-BabyMamba-HAR achieves channel count independent computational complexity through early fusion. Both architectures incorporate weight tied bidirectional scanning and context gated temporal attention pooling.

Through evaluation across eight diverse benchmarks, it is demonstrated that Crossover-BiDir-BabyMamba-HAR achieves 86.52% average macro F1-score with \sim 27K parameters and 2.21M average MACs, matching established baselines while offering 11 \times computational reduction on high channel datasets. Systematic ablations establish that bidirectionality (up to +8.42% F1-score) and gated attention (up to +8.94% F1-score) are critical components, while hyperparameters show remarkable robustness in the lightweight regime.

These findings provide practical guidance for deploying selective state space models as TinyML backbones for human activity recognition. Future work includes exploration of streaming variants, mixed stems for grouped sensors, and quantization aware training for microcontroller deployment.

REFERENCES

- [1] A. Gu and T. Dao, “Mamba: Linear-Time Sequence Modeling with Selective State Spaces,” *arXiv preprint arXiv:2312.00752*, 2023.
- [2] A. Gu, K. Goel, and C. Ré, “Efficiently Modeling Long Sequences with Structured State Spaces,” in *Proc. Int. Conf. Learning Representations (ICLR)*, 2022.
- [3] A. Vaswani, N. Shazeer, N. Parmar, J. Uszkoreit, L. Jones, A. N. Gomez, Ł. Kaiser, and I. Polosukhin, “Attention Is All You Need,” in *Advances in Neural Information Processing Systems*, vol. 30, 2017.

[4] F. J. Ordóñez and D. Roggen, "Deep Convolutional and LSTM Recurrent Neural Networks for Multimodal Wearable Activity Recognition," *Sensors*, vol. 16, no. 1, p. 115, 2016.

[5] Y. Zhou, H. Zhao, Y. Huang, T. Riedel, and M. Beigl, "TinyHAR: A Lightweight Deep Learning Model Designed for Human Activity Recognition," in *Proc. ACM Int. Symp. Wearable Computers (ISWC)*, 2022, pp. 89–93.

[6] S. Bian, M. Liu, V. F. Rey, D. Geissler, and P. Lukowicz, "TinierHAR: Towards Ultra-Lightweight Deep Learning Models for Efficient Human Activity Recognition on Edge Devices," in *Proc. ACM Int. Symp. Wearable Computers (ISWC)*, 2025, pp. 163–169.

[7] I. Loshchilov and F. Hutter, "Decoupled Weight Decay Regularization," in *Proc. Int. Conf. Learning Representations (ICLR)*, 2019.

[8] A. C. Muhoza, E. Bergeret, C. Brdys, and F. Gary, "Power Consumption Reduction for IoT Devices Thanks to Edge-AI: Application to Human Activity Recognition," *Internet of Things*, vol. 24, p. 100930, 2023.

[9] D. Geissler, D. Nshimyimana, V. F. Rey, S. Suh, B. Zhou, and P. Lukowicz, "Beyond Confusion: A Fine-grained Dialectical Examination of Human Activity Recognition Benchmark Datasets," *arXiv preprint arXiv:2412.09037*, 2024.

[10] S. Deng, J. Chen, D. Teng, C. Yang, D. Chen, T. Jia, and H. Wang, "LHAR: Lightweight Human Activity Recognition on Knowledge Distillation," *IEEE J. Biomed. Health Inform.*, 2023.

[11] W.-S. Lim, W. Seo, D.-W. Kim, and J. Lee, "Efficient Human Activity Recognition Using Lookup Table-Based Neural Architecture Search for Mobile Devices," *IEEE Access*, vol. 11, pp. 71727–71738, 2023.

[12] Y. Zhou, T. King, H. Zhao, Y. Huang, T. Riedel, and M. Beigl, "MLPHAR: Boosting Performance and Efficiency of HAR Models on Edge Devices with Purely Fully Connected Layers," in *Proc. ACM Int. Symp. Wearable Computers (ISWC)*, 2024, pp. 133–139.

[13] E. Lattanzi, L. Calisti, and C. Contoli, "Are Transformers a Useful Tool for Tiny Devices in Human Activity Recognition?," in *Proc. Int. Conf. Advances in Artificial Intelligence (ICAAI)*, 2024, pp. 339–344.

[14] Z. Hong, Z. Li, S. Zhong, W. Lyu, H. Wang, Y. Ding, T. He, and D. Zhang, "CrossHAR: Generalizing Cross-Dataset Human Activity Recognition via Hierarchical Self-Supervised Pretraining," *Proc. ACM Interact. Mob. Wearable Ubiquitous Technol.*, vol. 8, no. 2, pp. 1–26, 2024.

[15] S. Li, T. Zhu, F. Duan, L. Chen, H. Ning, C. Nugent, and Y. Wan, "HARMamba: Efficient and Lightweight Wearable Sensor Human Activity Recognition Based on Bidirectional Mamba," *arXiv preprint arXiv:2403.20183*, 2024.

[16] N. Y. Hammerla, S. Halloran, and T. Plötz, "Deep, Convolutional, and Recurrent Models for Human Activity Recognition Using Wearables," *arXiv preprint arXiv:1604.08880*, 2016.

[17] V. S. Murahari and T. Plötz, "On Attention Models for Human Activity Recognition," in *Proc. ACM Int. Symp. Wearable Computers (ISWC)*, 2018, pp. 100–103.

[18] D. Anguita, A. Ghio, L. Oneto, X. Parra, and J. L. Reyes-Ortiz, "A Public Domain Dataset for Human Activity Recognition Using Smartphones," in *Proc. European Symp. Artificial Neural Networks (ESANN)*, 2013.

[19] M. Malekzadeh, R. G. Clegg, A. Cavallaro, and H. Haddadi, "Mobile Sensor Data Anonymization," in *Proc. ACM/IEEE Int. Conf. Internet of Things Design and Implementation (IoTDI)*, 2019.

[20] J. R. Kwapisz, G. M. Weiss, and S. A. Moore, "Activity Recognition Using Cell Phone Accelerometers," *ACM SIGKDD Explorations Newsletter*, vol. 12, no. 2, pp. 74–82, 2011.

[21] A. Reiss and D. Stricker, "Introducing a New Benchmarked Dataset for Activity Monitoring," in *Proc. IEEE Int. Symp. Wearable Computers (ISWC)*, 2012, pp. 108–109.

[22] R. Chavarriaga, H. Sagha, A. Calatroni, S. T. Digumarti, G. Tröster, J. del R. Millán, and D. Roggen, "The Opportunity Challenge: A Benchmark Database for On-Body Sensor-Based Activity Recognition," *Pattern Recognition Letters*, vol. 34, no. 15, pp. 2033–2042, 2013.

[23] D. Micucci, M. Mobilio, and P. Napoletano, "UniMiB SHAR: A Dataset for Human Activity Recognition Using Acceleration Data from Smartphones," *Applied Sciences*, vol. 7, no. 10, p. 1101, 2017.

[24] P. Zappi, C. Lombriser, T. Stiefmeier, E. Farella, D. Roggen, L. Benini, and G. Tröster, "Activity Recognition from On-Body Sensors: Accuracy-Power Trade-Off by Dynamic Sensor Selection," in *Proc. European Conf. Wireless Sensor Networks (EWSN)*, Springer, 2008, pp. 17–33.

[25] M. Bächlin, M. Plotnik, D. Roggen, I. Maidan, J. M. Hausdorff, N. Giladi, and G. Tröster, "Wearable Assistant for Parkinson's Disease Patients with the Freezing of Gait Symptom," *IEEE Trans. Inf. Technol. Biomed.*, vol. 14, no. 2, pp. 436–446, 2010.

[26] M. Bock, A. Hölzemann, M. Moeller, and K. Van Laerhoven, "Improving Deep Learning for HAR with Shallow LSTMs," in *Proc. ACM Int. Symp. Wearable Computers (ISWC)*, 2021, pp. 7–12.

[27] A. Abedin, M. Ehsanpour, Q. Shi, H. Rezatofighi, and D. C. Ranasinghe, "Attend and Discriminate: Beyond the State-of-the-Art for Human Activity Recognition Using Wearable Sensors," *Proc. ACM Interact. Mob. Wearable Ubiquitous Technol.*, vol. 5, no. 1, pp. 1–22, 2021.

[28] C. I. Tang, I. Perez-Pozuelo, D. Spathis, S. Brage, N. Wareham, and C. Mascolo, "SelfHAR: Improving Human Activity Recognition Through Self-Training with Unlabeled Data," *arXiv preprint arXiv:2102.06073*, 2021.

[29] S. Zhang, Y. Li, S. Zhang, F. Shahabi, S. Xia, Y. Deng, and N. Alshurafa, "Deep Learning in Human Activity Recognition with Wearable Sensors: A Review on Advances," *Sensors*, vol. 22, no. 4, p. 1476, 2022.

[30] D. P. Kingma and J. Ba, "Adam: A Method for Stochastic Optimization," *arXiv preprint arXiv:1412.6980*, 2014.